Supporting Information

Allosteric communication disrupted by small molecule binding to the Imidazole glycerol phosphate synthase protein-protein interface.

Ivan Rivalta[§,#], George P. Lisi[#], Ning-Shiuan Snoeberger[#], Gregory Manley[#], J. Patrick Loria*[#,‡] and Victor S. Batista*[#]*

[§]Univ Lyon, Ens de Lyon, CNRS, Université Lyon 1, Laboratoire de Chimie UMR 5182, F-69342, Lyon, France. [#]Department of Chemistry and [‡]Department of Molecular Biophysics and Biochemistry Yale University, P.O. Box 208107, New Haven, CT 06520-8107, USA.

Table of content

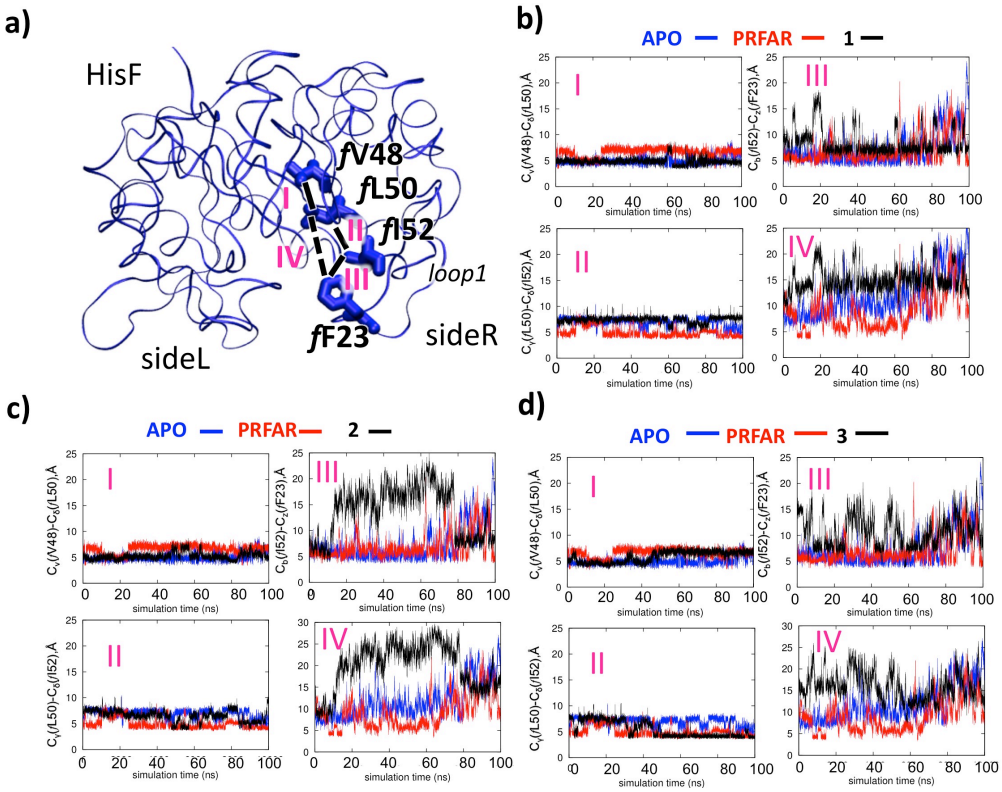

Figure S1. Hydrophobic contacts at the bottom of the HisF barrel in the apo, PRFAR-bound binary and ternary complexes. The distances (in Å) between amino acid residues with hydrophobic side chains, i.e. *f*F23, *f*V48, *f*L50 and *f*I52 (a), are monitored along the 0.1 μs MD simulations of the apo (blue), binary PRFAR-bound (red) and the ternary complexes (in black) with potential inhibitors **1-3** (b-d).

Table S1. Average distances (in Å) between hydrophobic amino acid residues at the bottom of the HisF barrel in the apo, PRFAR-bound binary and ternary complexes. The hydrophobic contacts defining the measured distances (with Roman numerals) are defined in Figure S1.

	apo	***PRFAR***	**1**	**2**	**3**
(I) fV48-fL50	5.02	*6.58*	*4.84*	*5.24*	*5.86*
(II) fL50-fI52	6.97	*5.02*	*7.40*	*6.47*	*5.45*
(III) fI52-fF23	*7.23*	*6.98*	*8.54*	*13.85*	*10.57*
(IV) fL50-fF23	*11.77*	*8.91*	*14.99*	*19.97*	*15.86*
(II)+(III)+(IV)	*25.79*	*20.91*	*30.93*	*40.29*	*31.88*

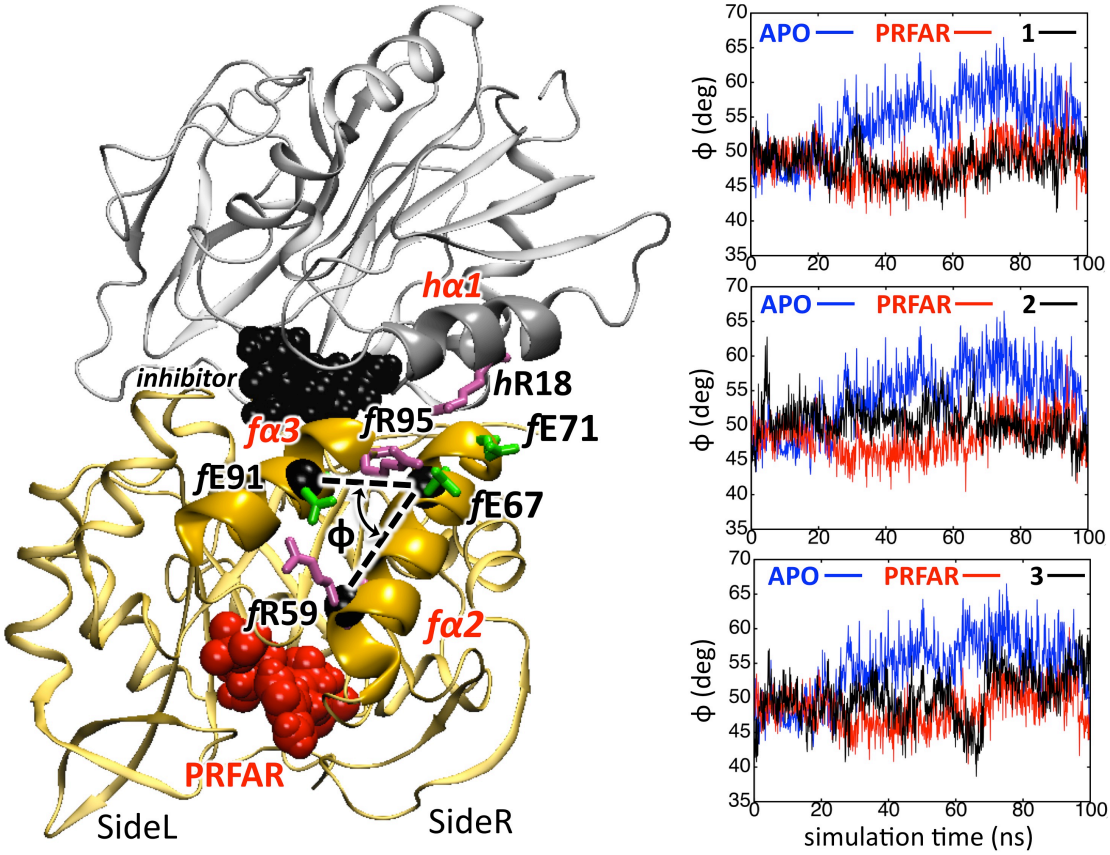

Figure S2. Relative positions of the *f*α2 and *f*α3 helices in the apo, PRFAR-bound binary and ternary complexes. The charged amino acid residues in the *f*α2 and *f*α3 helices are involved in specific contacts (left panel) that induce different relative positions of the two helices in the apo and PRFAR-bound complexes, taking an active part in the IGPS allosteric mechanism. The relative positions of the two helices are monitored (right panels) in along the 0.1 μs MD simulations of the apo (blue), binary PRFAR-bound (red) and the ternary complexes (in black) with potential inhibitors **1**-**3**.

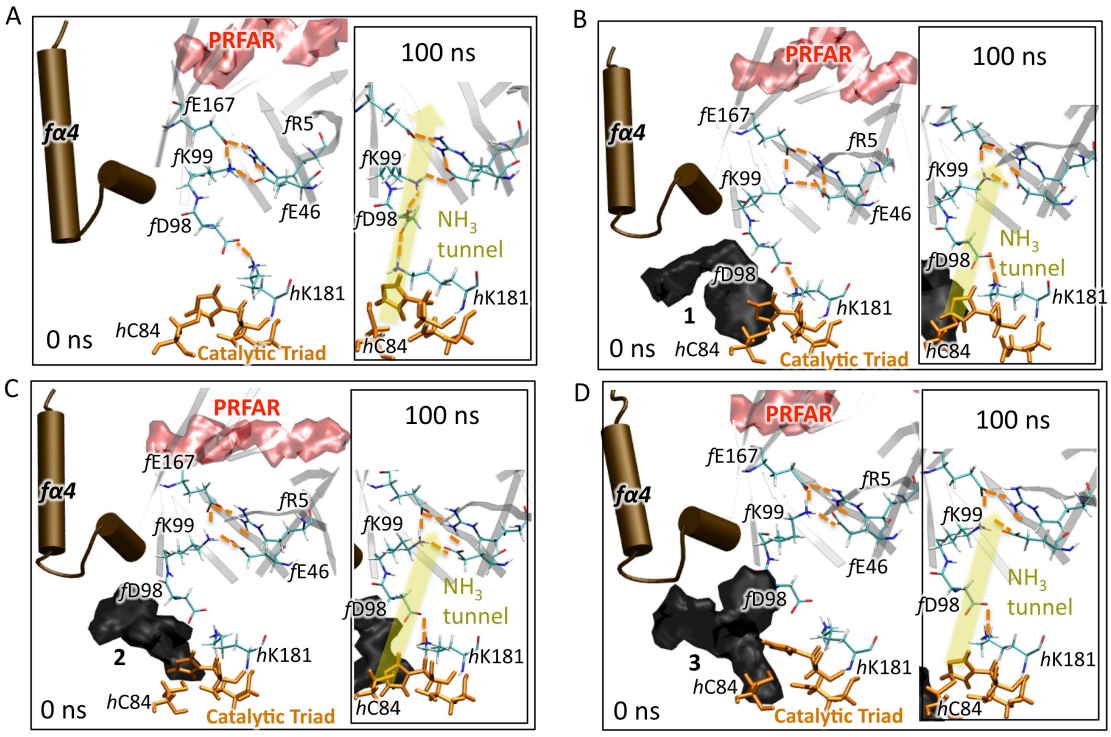

Figure S3. The influence of the inhibitor binding on the ammonia gate. Residues *f*R5, *f*E46, *f*K99, and *f*E167 create salt bridges that serve as ammonia gate for the HisF $(\beta/\alpha)_8$ barrel that opens within 100 ns in the MD trajectory of the PRFAR-bound binary complex (A), as expected for an active IGPS conformation, due to interactions between *f*K99 and *f*D98 side chains. When the inhibitors **1**-**3** bind (B-D) the gate remain closed due to the altered dynamics of *f*D98 induced by the interfacial ligands.

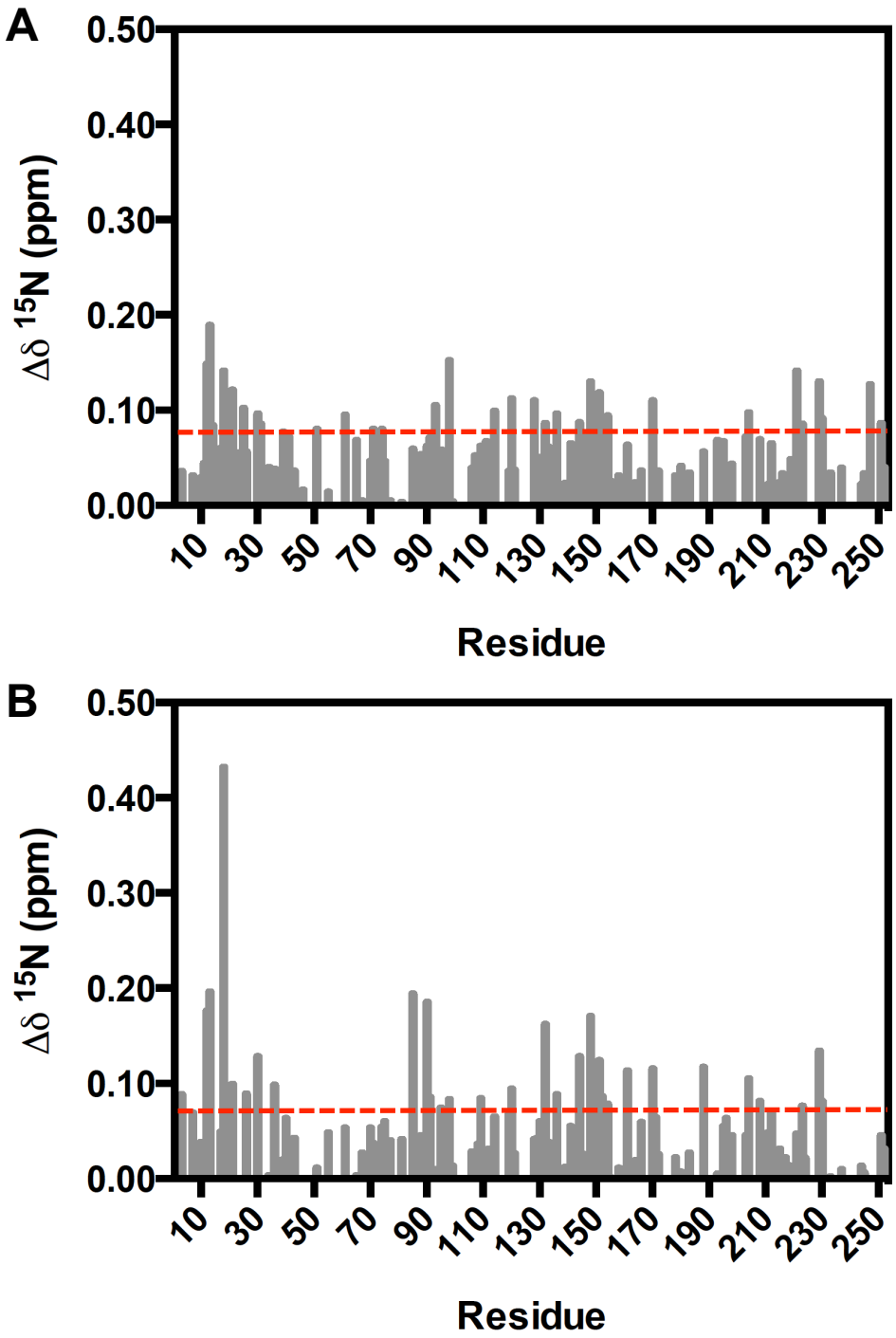

Figure S4. Chemical shift perturbations in the HisF domain of (A) apo IGPS and (B) PRFAR-bound IGPS upon titration with 3. The red line represents the 10% trimmed mean of all shifts, and perturbations greater than this cutoff are deemed significant.

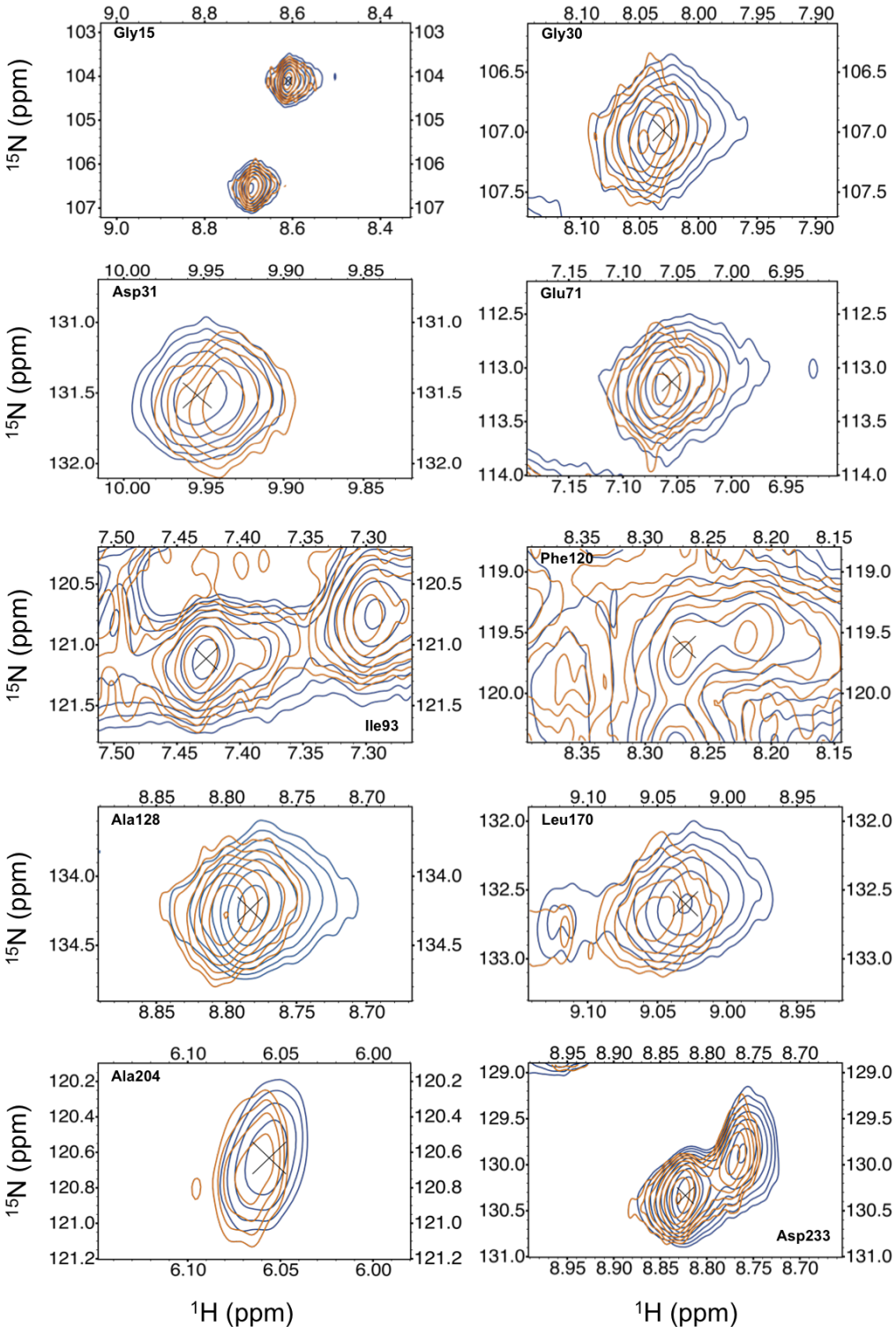

Figure S5. Representative correlation peaks from ^{1}H-^{15}N HSQC NMR experiments of ^{15}N-labeled HisF-IGPS. Titration of **3** into apo IGPS (blue) to a concentration of 3.17 mM (orange) causes distinct shifts in several resonances (Gly30, Asp31, Glu71, etc), while others remain unchanged (Gly15, Ile93). Significant chemical shift differences (Δδ) are summarized in Figure S6.

*f*Lys13	0.189
*f*Asp98	0.152
*f*Val12	0.145
*f*Val18	0.141
*f*Ala221	0.140
*f*Asn148	0.130
*f*Phe229	0.130
*f*Asn247	0.127
*f*Thr21	0.121
*f*Ile151	0.118
*f*Phe120	0.112
*f*Ala128	0.110
*f*Leu170	0.110
*f*Ile93	0.105
*f*Asn25	0.102
*f*Thr114	0.099
*f*Ala204	0.097
*f*Gly30	0.096
*f*Gly136	0.096
*f*Thr61	0.095
*f*Arg154	0.094
*f*Arg230	0.091
*f*Ser144	0.087
*f*Gly20	0.086
*f*Lys132	0.086
*f*Glu251	0.086
*f*Asp31	0.085
*f*Ala223	0.085
*f*Asp51	0.080
*f*Glu71	0.080
*f*Asp74	0.080

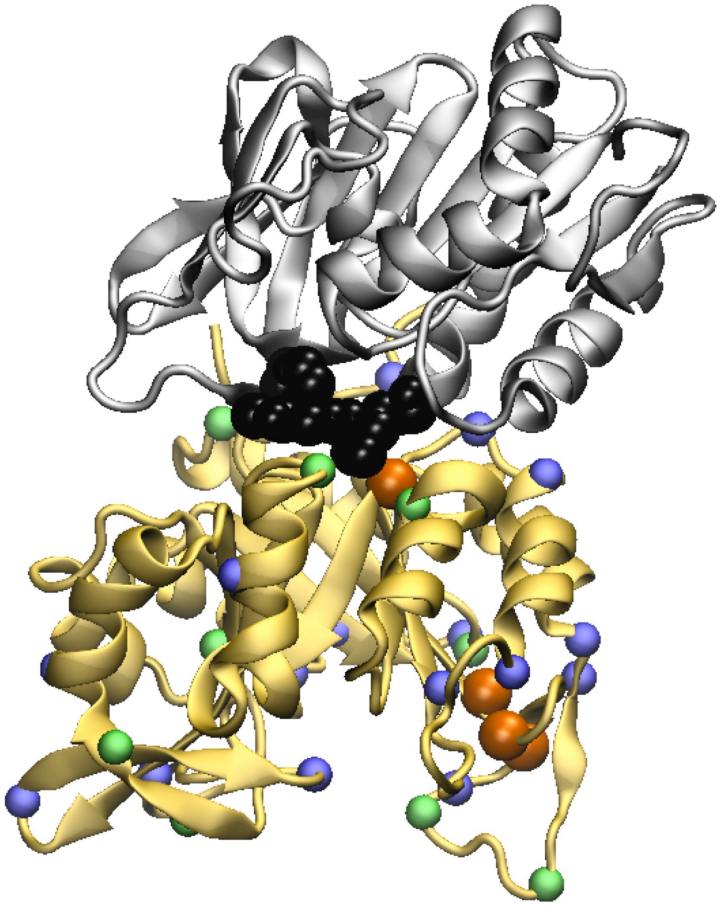

Figure S6. Chemical shifts changes in apo IGPS induced by binding of 3. Titration of **3** into apo IGPS (blue) to a concentration of 3.17 mM (orange) causes distinct shifts in several resonances (listed in the left panel). Residues with $\Delta\delta>0.14$ (orange balls at Cα), $\Delta\delta>0.10$ (light green) and $\Delta\delta>0.08$ (blue balls) are mapped onto the **3**-IGPS structure. Chemical shifts are determined by ^{1}H-^{15}N HSQC NMR experiments of ^{15}N-labeled HisF-IGPS.

Table S2. ^{15}N Chemical shift perturbations of HisH residues upon titration of apo IGPS with 3 (3.2 mM). Residues with Δδ >0.06 ppm were determined to be statistically significant from the 10% trimmed mean.

Residue	**Δδ (ppm)**
Arg18	0.092
Ser24	0.077
Ile32	*0.200*
Phe54	*0.051*
Gly55	*0.076*
Leu66	*0.061*
Phe69	*0.071*
Glu92	*0.140*
Glu95	*0.061*
Thr155	*0.065*
Arg200	*0.076*

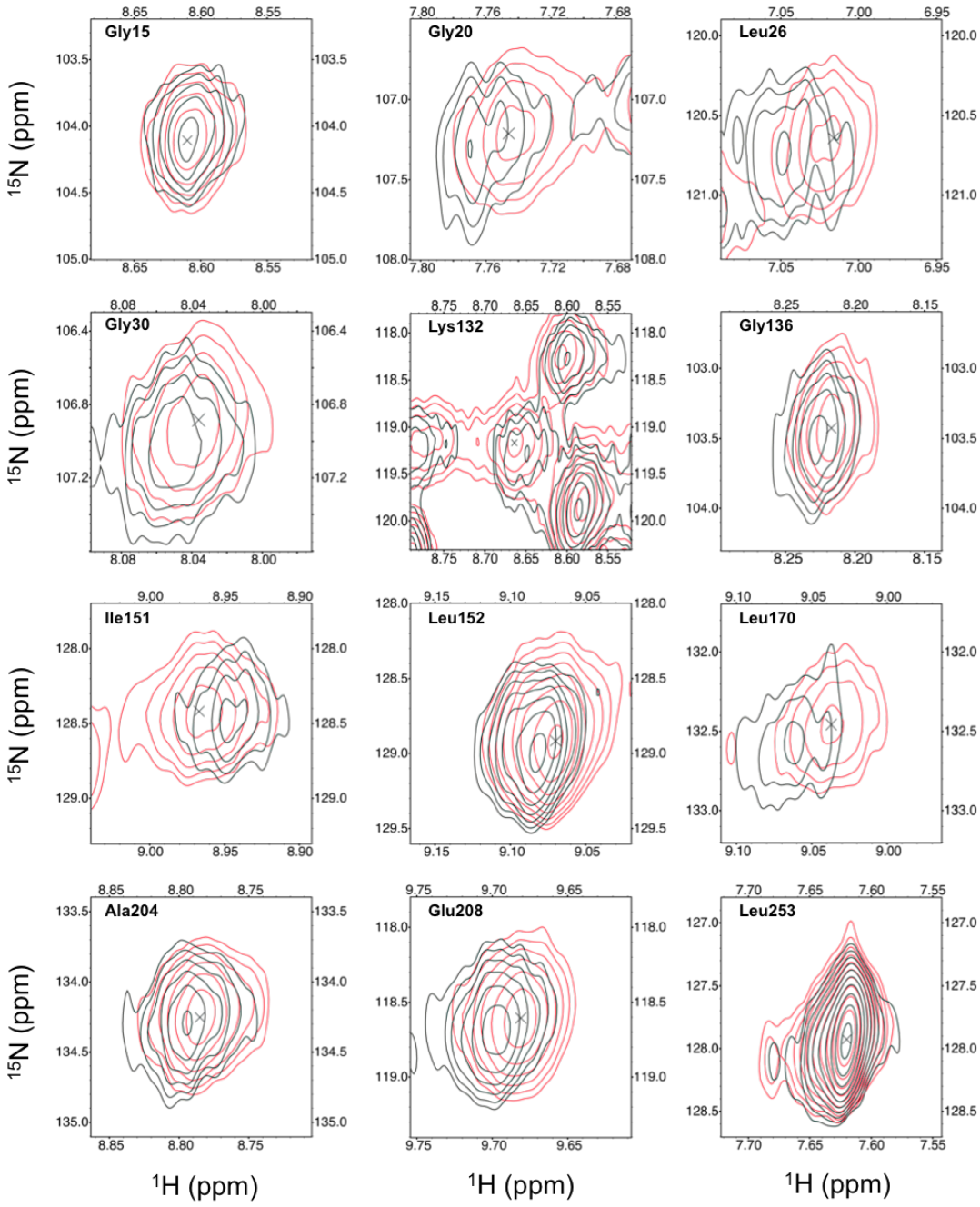

Figure S7. Representative correlation peaks from ^{1}H-^{15}N HSQC NMR experiments of ^{15}N-labeled HisF-IGPS. Titration of PRFAR into apo IGPS to a concentration of 0.96 mM (red) causes distinct shifts in several resonances, and titration of **3** into the binary complex to a concentration of 9.2 mM (black) causes further perturbation. Significant chemical shift differences (Δδ) are summarized in Figure S8.

Val18	0,432
Lys13	0,196
Asp85	0,194
Ser90	0,185
Val12	0,176
Lys132	0,162
Phe229	0,134
Gly30	0,128
Ser144	0,128
Ile151	0,124
Arg188	0,117
Leu170	0,115
Glu161	0,113
Ala204	0,105
Thr21	0,099
Gly36	0,098
Gly20	0,095
Phe120	0,094
Leu26	0,089
Ala3	0,088
Gly136	0,088
Leu152	0,086
Glu91	0,085
Asn109	0,084
Asp98	0,083
Glu208	0,081
Arg230	0,081

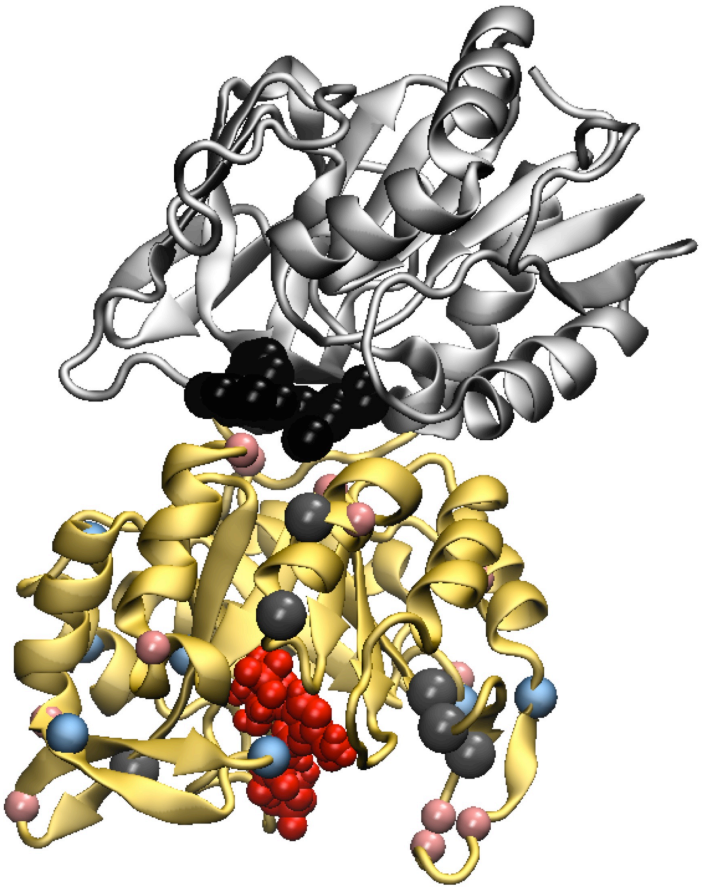

Figure S8. Chemical shifts changes in PRFAR-bound IGPS induced by binding of 3. Titration of **3** into binary IGPS (red) to a concentration of 9.2 mM (grey) causes distinct shifts in several resonances (listed in the left panel). Residues with Δδ>0.14 (grey balls), Δδ>0.10 (light blue) and Δδ>0.08 (pink balls) are mapped onto the 3-IGPS structure. Chemical shifts are determined by ^{1}H-^{15}N HSQC NMR experiments of ^{15}N-labeled HisF of the binary IGPS complex, with PRFAR concentration of 0.96 mM.

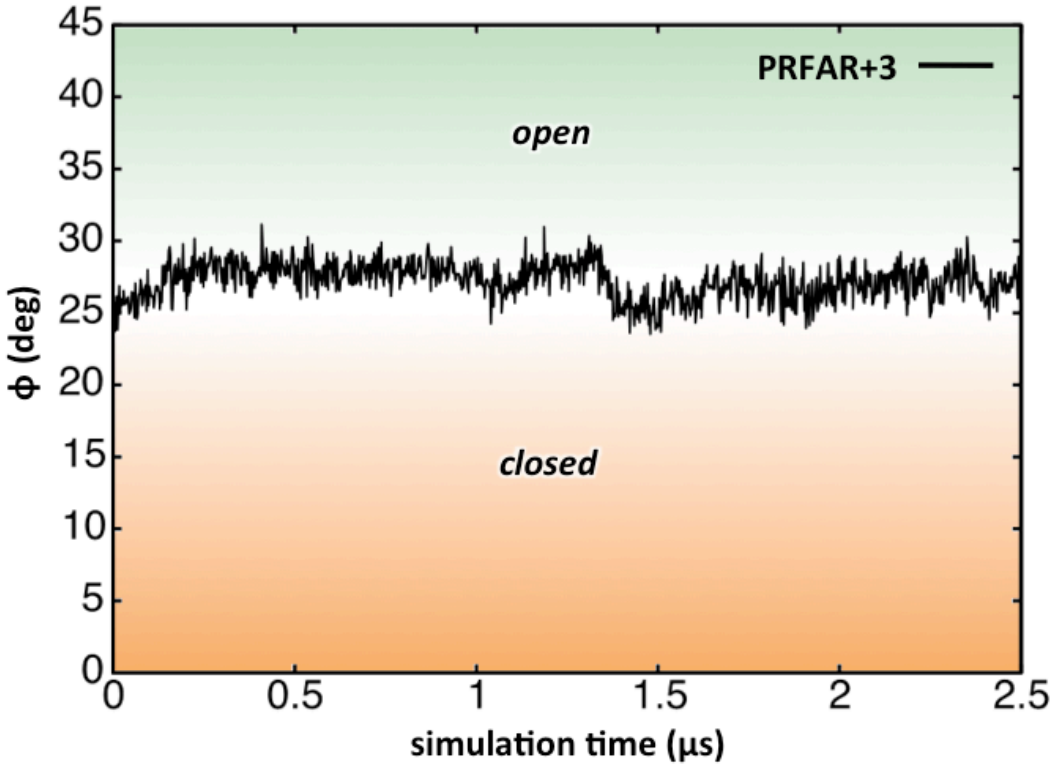

Figure S9. Breathing motion of the PRFAR-bound 3-IGPS ternary complexes. The breathing motion is measured by the angle (ϕ) defined by the Cα of the *f*F120, *h*W123 and *h*G52 (see main text). The evolution of ϕ during the MD simulation time (0-2.5 μs) is reported.